Electronic Supplementary Material (ESI) for Nanoscale.


# Supporting Information

# An engineered cascade-sensitized red-emitting upconversion nanoplatform with a tandem hydrophobic hydration-shell and metal-phenolic network decoration for single 808 nm triggered simultaneous tumor PDT and PTT enhanced CDT

Yameng Li,†[a] Yingjie Ding,†[a] Yifan Zhang,†[a] Zhiyue Sun,[b] Jiao Liu,[a] Mengxia Dai,[a,b] Jiayi Feng,[a] Bin Li,[b] Chaozhan Wang,[a] Yinmao Wei [a] and Ji-Wei Shen*[a]

[a] Key Laboratory of Synthetic and Natural Functional Molecule of the Ministry of Education. College of Chemistry & Materials Science, Northwest University, Xi'an 710127, P. R. China.

[b] Key Laboratory of Resource Biology and Biotechnology in Western China, Ministry of Education, School of Medicine, Northwest University, Xi'an 710069, P. R. China

† These authors contributed equally to this work.

* Corresponding author. E-mail: jiweish@nwu.edu.cn.

**Preparation of $NaErF_4$: Yb/Tm(69/1%):**

The $NaErF_4$:Yb/Tm(69/1%) core was synthesized through binary solvothermal method. In brief, 0.6 mmol of corresponding rare-earth acetates (30 mol% $Er(CH_3COO)_3$, 69 mol% $Yb(CH_3COO)_3$, 1 mol% $Tm(CH_3COO)_3$), 3.6 mL OA and 9 mL ODE were mixed in a 50 mL three-necked bottle. The system was heated to 160°C and reacted at this temperature for 30 min under argon protection. After the reaction solution cooled down, 1.30 mmol of NaOA was added and stirred for 10 min before adding 6 mL of methanol solution containing 0.2 mmol of NaOH and 2.4 mmol of $NH_4F$. The reaction solution was stirred for 30 min, then heated to 100 °C to evaporate the low-boiling point solvents. Finally, the reaction solution was heated to 300 °C and reacted at this temperature for 60 min. Upon cooling to room temperature, the as-formed core nanoparticles of $NaErF_4$:Yb/Tm(69/1%) were purified and re-dispersed in 6 mL of cyclohexane.

Synthesis of $NaErF_4$:Yb/Tm(69/1%)@$NaLuF_4$:Yb(*x*%). Typically, 0.3 mmol of corresponding rare-earth acetates (*x*% $Yb(CH_3COO)_3$, (100-*x*)% $Lu(CH_3COO)_3$), 3 mL of OA and 6 mL of ODE were mixed in a 50 mL three-necked bottle. Then, the resulting mixture was heated to 150 °C and reacted for 60 min under argon protection. After the mixture was cooled down to 50 °C, 3 mL of the as-prepared $NaErF_4$:Yb/Tm(69/1%) core nanoparticles in cyclohexane were added. Thereafter, 5 mL methanol solution containing NaOH (0.75 mmol) and $NH_4F$ (1.2 mmol) was added dropwisely. After vigorous stirring at 50 °C for 30 min, the low-boiling point solvents in the reaction system were evaporated by heating to 100 °C. Subsequently, the reaction system heated to 300 °C and reacted at this temperature for 1 h under argon protection. Upon cooling to room temperature, the as-formed $NaErF_4$:Yb/Tm(69/1%)@$NaLuF_4$:Yb(*x*%) nanoparticles were purified and re-dispersed in 3 mL of cyclohexane.

Preparation of core/multi-shell structured $NaErF_4$:Yb/Tm(69/1%)@ $NaLuF_4$:Yb($x$%)@$NaLuF_4$:Nd/Yb(20/10%), $NaErF_4$:Yb/Tm(69/1%)@$NaLuF_4$:Yb(15%)@ $NaLuF_4$:Nd/Yb($x$/10%) and $NaErF_4$:Yb/Tm(69/1%)@$NaLuF_4$:Yb(15%)@ $NaLuF_4$:Nd/Yb(30/10%)@$NaLuF_4$. The synthesis procedures are identical to those of in preparing core/shell structured $NaErF_4$:Yb/Tm(69/1%)@$NaLuF_4$:Yb($x$%) nanoparticles. Particularly, thicker sensitization layer ($NaLuF_4$:Yb(15%)) and inert shell ($NaLuF_4$) were achieved by increasing the rare-earth amounts in preparing the corresponding shell growth stock solutions.

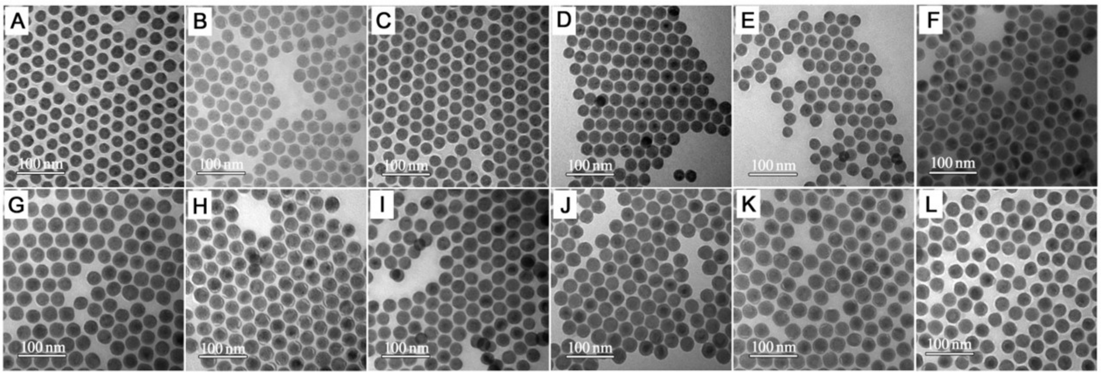


**Fig. S1** TEM images of the $NaErF_4$:Yb/Tm(69/1%)@$NaLuF_4$:Yb($x$%) (A-F) and corresponding energy sensitization layer ($NaLuF_4$:Nd/Yb(20/10%)) coated $NaErF_4$:Yb/Tm(69/1%)@ $NaLuF_4$:Yb($x$%) (G-L), respectively. The $Yb^{3+}$ doping ratios ($x$%) are 2.5%, 5%, 10%, 15%, 20% and 30% for the samples used in (A, G), (B, H), (C, I), (D, J), (E, K) and (F, L), respectively.

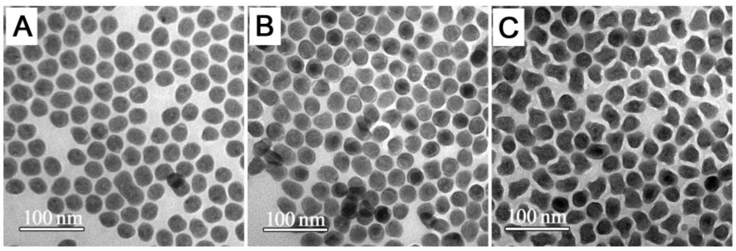


**Fig. S2** TEM images of $NaErF_4$:Yb/Tm(69/1%)@$NaLuF_4$:Yb(15%)@$NaLuF_4$:Nd/Yb($x$/10%). The $Nd^{3+}$ doping ratios ($x$%) are 30%, 40% and 50% for the samples used in (A), (B) and (C), respectively. The sensitization layer thickness in the $NaErF_4$:Yb/Tm(69/1%)@ $NaLuF_4$:Yb(15%)@$NaLuF_4$:Nd/Yb(30/10%) is ~1.1 nm.

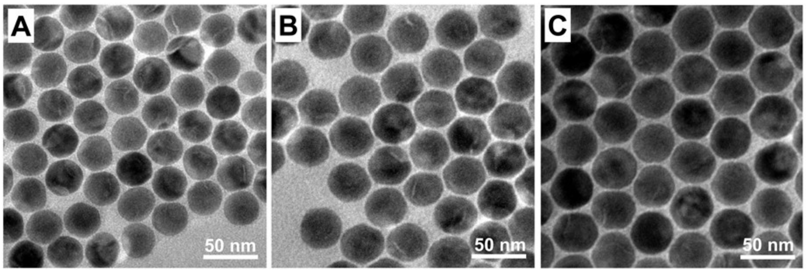


**Fig. S3** TEM images of $NaErF_4$:Yb/Tm(69/1%)@$NaLuF_4$:Yb(15%)@$NaLuF_4$:Nd/Yb(30/10%) @$NaLuF_4$ with different inter shell ($NaLuF_4$) thickness: (A) 1.5 nm, (B) 3.0 nm, (C) 5.0 nm.

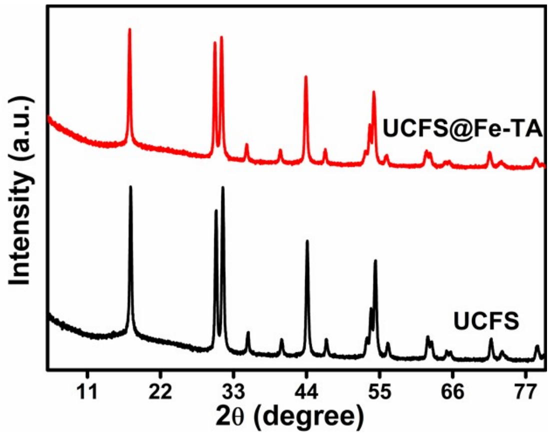


**Fig. S4** X-ray diffraction patterns of the UCFS and UCFS@Fe-TA.

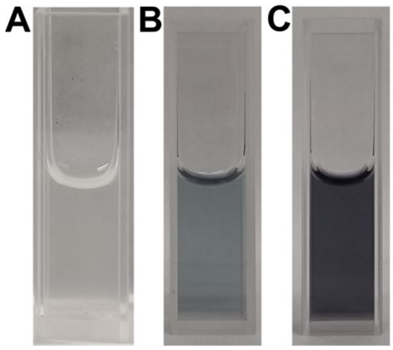


**Fig. S5** Photographs of the US (A), UCFS (B) and UCFS@Fe-TA (C).

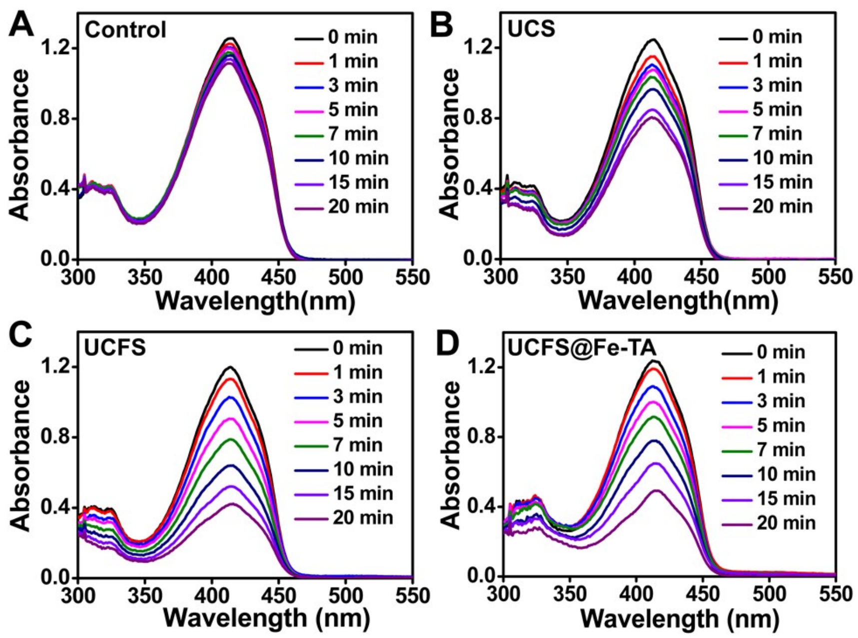


**Fig. S6** Time-dependent DPBF depletion capacity of the UCS, UCFS and UCFS@Fe-TA under 808 nm irradiation (2 W $cm^{-2}$).

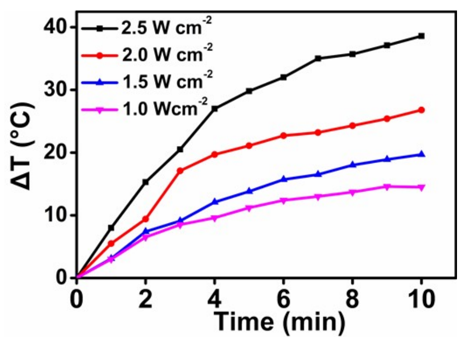


**Fig. S7** NIR irradiation power density-dependent temperature rise characteristic of the aqueous UCFS@Fe-TA (0.25 mg $mL^{-1}$).

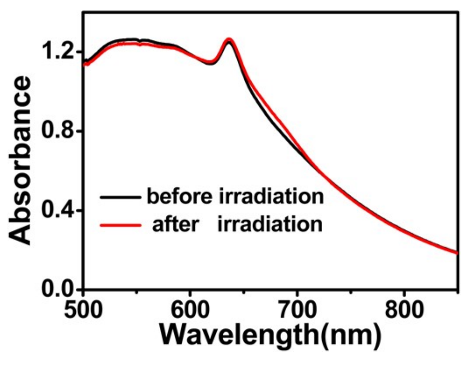


**Fig. S8** The absorbance change of UCFS@Fe-TA after continuous five circles of 808 nm irradiation.

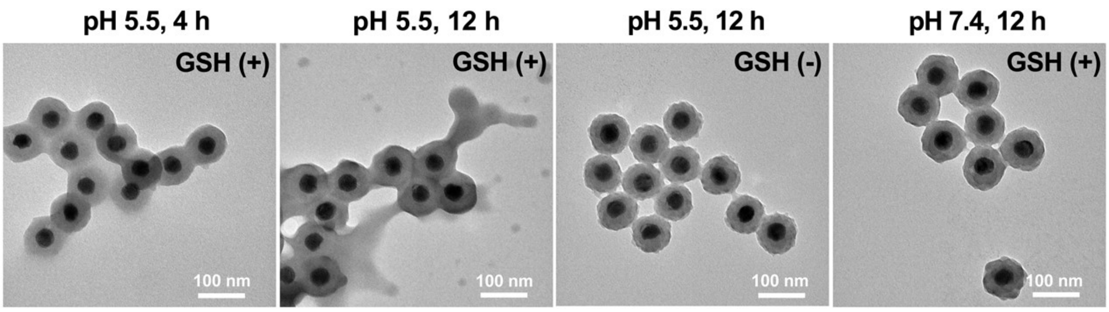


**Fig. S9** TEM observations of the Fe-TA dissociation on the surface of UCFS at different time and under different conditions. Results suggest Fe-TA will dissociate under acidic conditions in the presence of GSH.

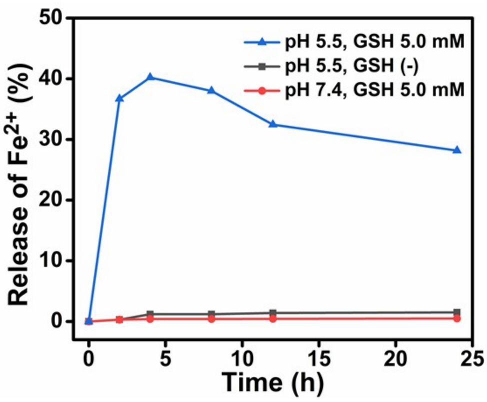


**Fig. S10** Evaluation of the Fe-TA dissociation on the surface of UCFS at different time and under different conditions by using *o*-phenanthroline method. Results suggest Fe-TA will dissociate under acidic conditions in the presence of GSH.

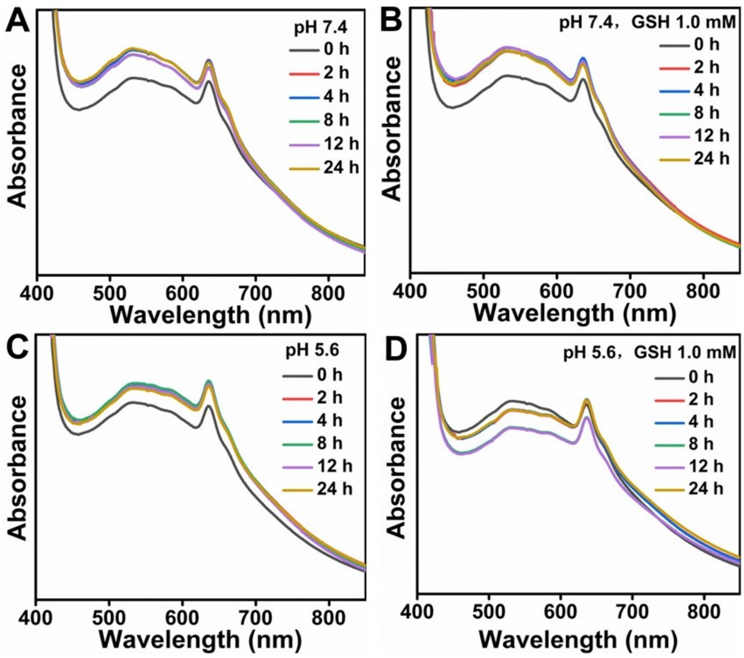


**Fig. S11** UV-vis spectra of UCFS@Fe-TA after incubation in acidic conditions with or without GSH addition. Results suggested that the absorbance of UCFS@Fe-TA showed significant increase in neutral conditions even with GSH addition (Fig. S11A-B), and also significant increase in acidic conditions without GSH addition (Fig. S11C). The absorbance of UCFS@Fe-TA decreased in acidic conditions with GSH addition at 8~12 h, however, increase back up to the original level at 24 h (Fig. S11D). Upon GSH was consumed completely, the $Fe^{2+}$ might convert back to $Fe^{3+}$ due to the oxidation effect of dissolved $O_2$ in water (Fig. S11D). The NIR absorption capacity loss of UCFS@Fe-TA in acidic conditions with GSH addition is limited, indicating the Fe-TA dissociation and reliable PTT of Fe-TA are not in conflict.

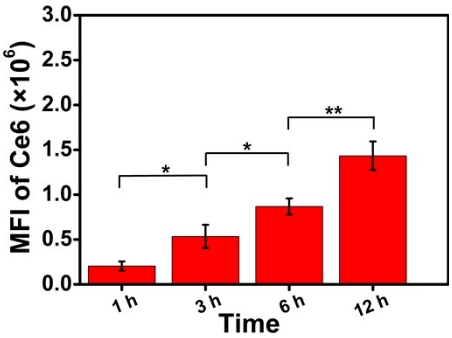


**Fig. S12** Mean fluorescence intensity (MFI) of Ce6 in MCF-7 cells after incubating with UCFS@Fe-TA for different times. *$p < 0.05$, **$p < 0.01$ determined by Student's *t* test.

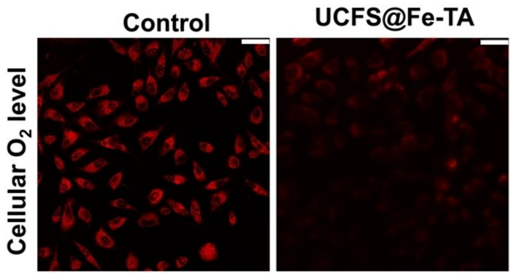


**Fig. S13** $O_2$ content evaluation in UCFS@Fe-TA treated MCF-7 cells by the intracellular $O_2$ level indicator $[Ru(dpp)_3]Cl_2$. The hypoxia nature of MCF-7 cells was relieved after incubating with UCFS@Fe-TA (12 h).

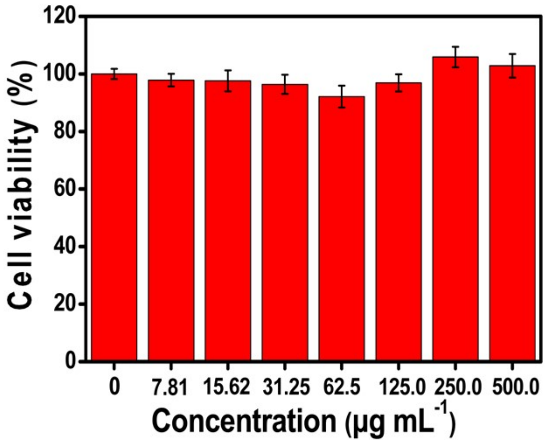


**Fig. S14** The viability of L929 cells after incubation with UCFS@Fe-TA for 24 h.

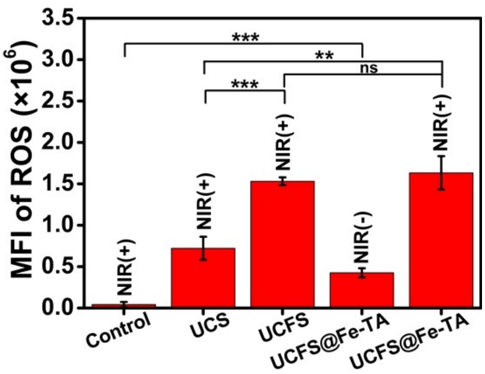


**Fig. S15** MFI of ROS in MCF-7 cells after treating by the as-involved nanoprobes. $^{**}p < 0.01$, $^{***}p < 0.001$ determined by Student's *t* test. ns, not significant ($p > 0.05$).

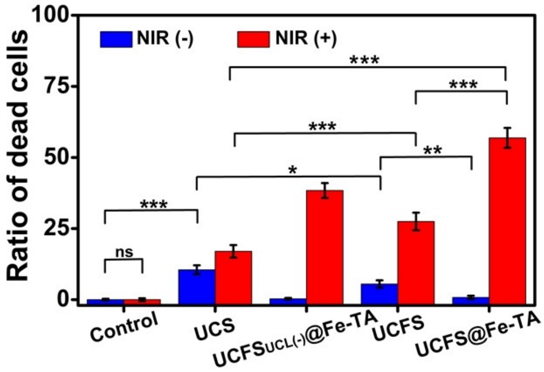


**Fig. S16** Ratio of dead cells calculated from the calcein-AM/PI cell double staining results. *$p < 0.05$, **$p < 0.01$, ***$p < 0.001$ determined by Student's *t* test. ns, not significant ($p > 0.05$).

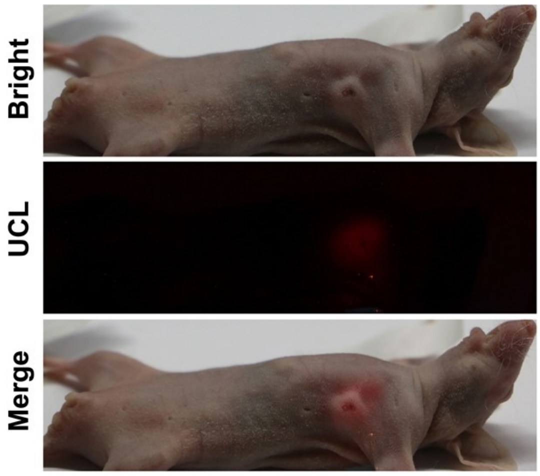


**Fig. S17** The UCL based in vivo imaging of tumor bearing mouse after iv injecting with the UCFS@Fe-TA for 12 h, demonstrating tumor accumulation of UCFS@Fe-TA.

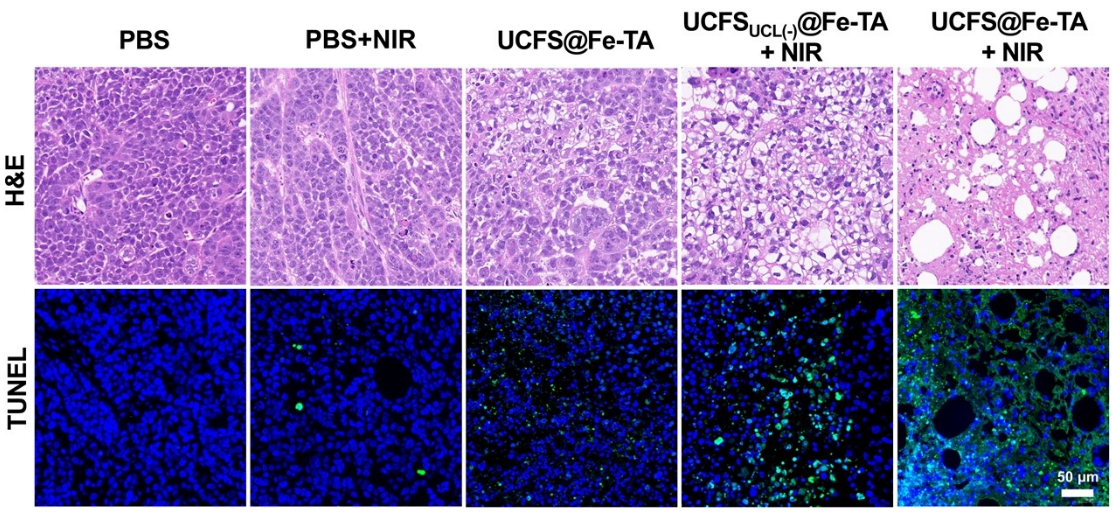


**Fig. S18** H&E and TUNEL staining images of tumor tissues after 14 days of treatments.